Nuclear Instruments and Methods in Physics Research B 361 (2015) 620–626

Contents lists available at ScienceDirect

Nuclear Instruments and Methods in Physics Research B

journal homepage: www.elsevier.com/locate/nimb

Accretion rate of extraterrestrial ^{41}Ca in Antarctic snow samples

J.M. Gómez-Guzmán [a,*], S. Bishop [a], T. Faestermann [a], N. Famulok [a], L. Fimiani [a], K. Hain [a], S. Jahn [a], G. Korschinek [a], P. Ludwig [a], D. Rodrigues [b]

[a] Technische Universität München, Fakultät für Physik, James-Franck-Strasse 1, 85748 Garching, Germany
[b] Laboratorio TANDAR, Comisión Nacional de Energía Atómica, Argentina

ARTICLE INFO

Article history:
Received 14 December 2014
Received in revised form 5 May 2015
Accepted 13 May 2015
Available online 22 May 2015

Keywords:
AMS
^{41}Ca
Interplanetary dust

ABSTRACT

Interplanetary Dust Particles (IDPs) are small grains, generally less than a few hundred micrometers in size. Their main source is the Asteroid Belt, located at 3 AU from the Sun, between Mars and Jupiter. During their flight from the Asteroid Belt to the Earth they are irradiated by galactic and solar cosmic rays (GCR and SCR), thus radionuclides are formed, like ^{41}Ca and ^{53}Mn. Therefore, ^{41}Ca ($T_{1/2} = 1.03 \times 10^5$ yr) can be used as a key tracer to determine the accretion rate of IDPs onto the Earth because there are no significant terrestrial sources for this radionuclide. The first step of this study consisted to calculate the production rate of ^{41}Ca in IDPs accreted by the Earth during their travel from the Asteroid Belt. This production rate, used in accordance with the $^{41}Ca/^{40}Ca$ ratios that will be measured in snow samples from the Antarctica will be used to calculate the amount of extraterrestrial material accreted by the Earth per year. There challenges for this project are, at first, the much longer time for the flight needed by the IDPs to travel from the Asteroid Belt to the Earth in comparison with the ^{41}Ca half-life yields an early saturation for the $^{41}Ca/^{40}Ca$ ratio, and second, the importance of selecting the correct sampling site to avoid a high influx of natural ^{40}Ca, preventing dilution of the $^{41}Ca/^{40}Ca$ ratio, the quantity measured by AMS.

1. Introduction

Interplanetary Dust Particles (IDPs) are small grains, generally less than a few hundred micrometers in size in orbit around the Sun. The main sources of extraterrestrial matter in our solar system are the Kuiper and the Asteroid Belt. The dust particles are produced by evaporation of the cometary material and collisions of asteroids induced by the strong gravitational field of Jupiter in the Asteroid Belt. Asteroids and comets contribute different fraction of material with different sizes. The size distribution of the dust particles encountering Earth peaks at about 200 μm in diameter [1]. The dust grains of less than 10 μm are lost from the solar system by way of accretion onto larger planets, such as Saturn and Jupiter, and also due to the solar wind [2]. The Poynting–Robertson drag [3] causes the dust particles from the Asteroid Belt and comets to spiral into the Sun.

Based on the analysis of IDPs sampled in the stratosphere, in deep sea sediments and in Antarctic ice, it has been proposed that the chemical composition of IDPs is similar to CM [4] or CI [5] chondrites.

While bodies are traveling through the solar system, they are irradiated by two kinds of high energy particles: galactic cosmic-rays (GCR) and solar cosmic-rays (SCR). The interaction of both GCR and SCR with cosmic dust, meteoroids and planetary surfaces produces a large variety of cosmogenic nuclides, among them, ^{41}Ca and ^{53}Mn.

The Earth's meteoritic accretion rate plays an important role in many contexts. Meteoroids entering the Earth's upper atmosphere deposit meteoritic matter there, a process which has important consequences for the aeronomy of the upper mesosphere and lower ionosphere since it may help to quantify the meteoroid collision hazards for spacecraft [6]. However, the annual flux of extraterrestrial material falling on Earth is still not well established, and it has been estimated between 220 and 78,000 tons per year [6, and references therein].

About 90% of the incoming mass of submillimeter extraterrestrial dust particles evaporates during atmospheric entry [7]. Thus the constituent minerals of these particles subsequently vaporize at altitudes between 80 and 120 km [8]. In this way, minerals are set free and can be measured by using aerosol and/or ice sampling techniques. Cosmic dust accumulates in oceanic sediments and areas with slow sedimentation rates such as Greenland or Antarctica [9].

* Corresponding author.
E-mail address: jose.gomez@ph.tum.de (J.M. Gómez-Guzmán).

http://dx.doi.org/10.1016/j.nimb.2015.05.016
0168-583X/

Calcium-41 is a nuclide of interest for studies of the irradiation history of extraterrestrial matter because its half-life of $T_{1/2} = 104 \pm 5$ kyr [10] fills the gap between those of ^{14}C ($T_{1/2} = 5.7$ kyr) and ^{36}Cl ($T_{1/2} = 300$ kyr). It is mainly produced in extraterrestrial objects by spallation reactions by GCR and SCR on the target materials Fe, Ni and Ti, and by neutron-capture reactions [53]. In the Earth's surface it is formed by thermal neutron capture ^{40}Ca(n,γ)^{41}Ca, leading to atomic ratios ^{41}Ca/^{40}Ca in the order of 10^{-15}, only measurable by Accelerator Mass Spectrometry (AMS). Thus, ^{41}Ca could be used as a key tracer for interplanetary dust as it has not significant terrestrial sources. A critical parameter for the application of ^{41}Ca as a tracer of extraterrestrial material is its rate of accretion.

The successful detection of ^{41}Ca in meteorites has been previously achieved in different AMS facilities around the world, like Rehovot [17,50], Rochester [51], Pennsylvania [11,14,16,53], Lawrence Livermore [19] and Munich [52,54,57].

The aim of this study is to show the production rate of ^{41}Ca in IDPs, due to their interaction with GCR and SCR, if the Asteroid Belt is assumed to be their main origin. Once this production rate is known, the accretion rate of extraterrestrial ^{41}Ca can be calculated and can be used as a new proxy to determine the annual deposition of extraterrestrial material on Earth. For this work, snow samples from different sampling stations in Antarctica were collected in order to measure the atomic ratio ^{41}Ca/^{40}Ca and thus, calculate the accretion rate of ^{41}Ca onto the Earth.

2. Reaction channels producing ^{41}Ca in Interplanetary Dust Particles

As stated by Fink et al. [11], there are three reaction channels which dominate ^{41}Ca production in extraterrestrial environments which are characterized by the energy of the bombarding nucleon and target species: (1) high-energy spallation by GCR on iron and nickel, (2) solar-proton-induced reactions on titanium and (3) thermal neutron capture on the most abundant stable Ca isotope, ^{40}Ca. The production of ^{41}Ca by neutron-capture reactions in large objects that later becomes small particles could be a major source of ^{41}Ca because rates for making ^{41}Ca by neutron capture on ^{40}Ca in large objects, like Allende meteoroid, can have rates of about 1500 dpm/kg-Ca [55].

For the production of ^{41}Ca in IDPs, two spallation processes are the most common and important; namely, ^{nat}Fe(p,x)^{41}Ca and ^{nat}Ni(p,x)^{41}Ca. The analytical expression for the calculation of the production rate P_i of any long-lived nuclide is given by:

$$P_i = \sum_j \int \frac{d\phi}{dE} \times N_j \times \sigma(j \to i, E)dE \quad (1)$$

where $\sigma(j \to i,E)$ is the relevant nuclear cross section as a function of energy, $\phi(E)$ represents the flux of incident particles as a function of the energy and N_j is the number of target atoms j (Fe or Ni).

As stated in Eq. (1), the production rates from different sources depend on the abundance of the target material N_j and on the spallation cross sections for both reactions. As shown by different authors [12,13], both reactions have very similar cross sections for a proton energy range of 100–1600 MeV. Therefore, the production rates will depend on the relative amount of target atoms in the dust. Taking into account that on average, IDPs with CI and CM chondritic composition contain about 17 times more (related to mass) iron than nickel [4,5,18], it can be concluded that ^{41}Ca is mainly produced by spallation on iron. Different authors [14–16] have calculated the production rate of ^{41}Ca for this channel at energies from 10 MeV to 10 GeV and reported a saturation activity of (24 ± 1) dpm kg^{-1} for the iron phase of meteorites. This value should be representative of the ^{41}Ca saturation (specific) activity for small meteorites of long exposure age and zero terrestrial age [17].

The production rate of ^{41}Ca due to thermal neutron-capture in diogenites is less than 0.01 dpm g(Ca)$^{-1}$ in objects less than 10 cm in radius as stated by Welten et al. [19]. In this work, only dust particles with much smaller radii are considered (maximum diameter of around 450 μm), because the contribution of larger particles to the terrestrial accretion is negligible [20]. Assuming that IDPs with CM and CI chondritic composition contain about 1% weight of ^{40}Ca [4,5,18], this corresponds to a production rate less than 0.1 dpm kg^{-1}sample.

With these results it is clear that the most important reaction channel for the production of extraterrestrial ^{41}Ca in IDPs is high-energy spallation reactions on iron, so this channel will be the only one used to calculate the production rate of ^{41}Ca in IDPs. This saturation activity of ^{41}Ca will be used in further sections to calculate the expected accretion rate of extraterrestrial ^{41}Ca onto the Earth.

3. Irradiation of IDPs in interplanetary space

Cosmic rays are classified into a solar and a galactic component (SCR and GCR respectively). The SCR component originates from our Sun and mainly (~90%) consists of protons [21]. The GCR component mainly (~87%) consists also of protons [21]. The second most abundant component in cosmic rays consists of α-particles followed by less than 1% of heavier nuclei [21].

Any discussion concerning the origin of IDPs accreted onto Earth implies an understanding of their motion in space. Forces acting on particles in our solar system are dominantly induced by the Sun. Besides the Sun's gravitational force, also non-gravitational forces such as scattering of light and interaction with solar wind particles contribute significantly. The scattering of solar light slows the particles down and lets their orbit decrease towards the Sun, removing them on time scales of 10^4 to 10^6 years. This is the so called Poynting–Robertson effect [3]. The interaction with solar wind particles also forces IDPs towards the Sun.

The formation of cosmogenic nuclides in the IDPs depends on the irradiation history of the particles and consequently on their age and orbital trajectories. A significant proportion of the IDPs accreted onto the Earth is believed originate from the Asteroid Belt, at about 3 AU ($1\ \text{AU} = 1.5 \times 10^{11}$ m) in our solar system. Consequently, the model for the production of a radionuclide explained in following sections and extracted from [22] considers particles originating (i.e. being formed) at 3 AU. After formation, the IDPs approach the Earth due to the combined action of solar gravitation and Poynting–Robertson effect. Other forces, for example gravitational influence from planets are not considered in the model. Changes in mass and size of IDPs during motion (for example because of collisions) are also neglected in the model.

The irradiation of the IDPs by cosmic rays is then described by a Bateman equation of radioactive decay of a nucleus with a production term due to a galactic component P_G and another due to the solar component P_S, as shown in Eq. (2),

$$\frac{1}{M_{sample}} \cdot \frac{dN(t)}{dt} = -\frac{\lambda}{M_{sample}} \cdot N(t) + P_G(t) + P_S(t) \quad (2)$$

where $N(t)$ is the number of atoms of the radionuclide of interest, λ is its decay constant and M_{sample} is the mass of the sample.

For a symmetric solar cosmic proton flux the solar production rate $P_S(t)$ is proportional to $1/a^2$, where a is the distance from the Sun. With this, the production rate $P_S(t)$ can be written as shown in Eq. (3),

$$P_S(t) = P_0 \cdot \left(\frac{a_e}{a(t)}\right)^2 \quad (3)$$

where P_0 is the production rate at 1 AU, a_e is 1 AU and $a(t)$ is the orbital distance of the IDPs as a function of time.

The orbital distance $a(t)$ as a function of time can be calculated if the IDPs are assumed to be predominantly formed in the Asteroid Belt: after formation, the IDPs are accelerated towards the Sun by the Poynting–Robertson light drag and solar wind drag. The equation of motion for a spherical particle on a circular heliocentric orbit under the force of the Poynting–Robertson light and solar wind drag is given by Eq. (4) [23],

$$\frac{da(t)}{dt} = \frac{-k}{a \cdot \rho \cdot r} \quad (4)$$

where k is a constant with value $1.3 \times 5.12 \times 10^{11}$, and ρ and r are the density and radius of the IDPs, respectively. The constant k is calculated based of some assumptions: (i) a solar wind drag of 30% of solar light drag; (ii) Mie-scattering coefficient of 1; and (iii) scattering and brake-up of IDPs during their pathway to Earth are neglected [1].

Considering the boundary condition $a_{(t=0)} = a_0 = 3$ AU, i.e. IDPs starting their travel from the Asteroid Belt, the integration of Eq. (4) yields the travel time of IDPs from the orbit of origin (a_0) to the orbit $a(t)$, as shown in Eq. (5).

$$t = \left[a_0^2 - a^2(t)\right] \cdot \frac{\rho \cdot r}{2k} \quad (5)$$

For spherical IDPs with a typical density of 2.5 g cm^{-3} [20] and 200 µm diameter, the time of flight to the Earth's orbit $a(t) = a_e = 1$ AU starting at an orbit a_0 of 3 AU as calculated by Eq. (5) is around a million years. The traveling time obtained with Eq. (5) can be compared to the one obtained by Kortenkamp and Dermott [1] as a result of the numerical solution of the full equations of motion of a 10 µm particle. Their simulations yield a traveling time of 52×10^3 years for a particle originating at approximately 3 AU, while the above equation yields a traveling time of 55×10^3 years, shows its validity for this study. Combining Eqs. (5) and (3), the production rate $P_S(t)$ can be rewritten as denoted by Eq. (6).

$$P_S(t) = P_0 \cdot \left(\frac{a_e}{a(t)}\right)^2 = P_0 \cdot \frac{a_e^2}{a_0^2 - \frac{2 \cdot k \cdot t}{\rho \cdot r}} \quad (6)$$

Using this result in Eq. (2) allows us to rewrite the equation that governs the irradiation of the IDPs by cosmic rays as shown in Eq. (7). Since the mean GCR proton spectrum in the meteoroid orbits has been constant over about the last 10 Myr [24] and its dependence on the distance from the Sun is only very minor [9], the distance and thus the time dependency of $P_G(t)$ is neglected in the irradiation model.

$$\frac{1}{M_{\text{sample}}} \cdot \frac{dN(t)}{dt} = -\frac{\lambda}{M_{\text{sample}}} \cdot N(t) + P_G + P_0 \cdot \frac{a_e^2}{a_0^2 - \frac{2 \cdot k \cdot t}{\rho \cdot r}} \quad (7)$$

Solving this differential equation from $t = 0$ to the time of flight given in Eq. (5) allows us to obtain the production rate in dependence of the IDPs radii r, assuming constant density ρ and a certain mass distribution of IDPs [20,25] shown in Fig. 1.

It should be noted that in the above calculation, the ^{41}Ca activity at the time of formation of the particles has not been taken into account. In the following sections it will be explained how to calculate both galactic and solar components of the production rate shown in Eq. (7). In the case of the galactic component, we have used ^{53}Mn as a proxy for ^{41}Ca since its concentration in IDPs is dominated by production by GCR and results essentially from spallation reactions involving iron isotopes. In the case of the solar component, results derived from applying the irradiation model will be shown.

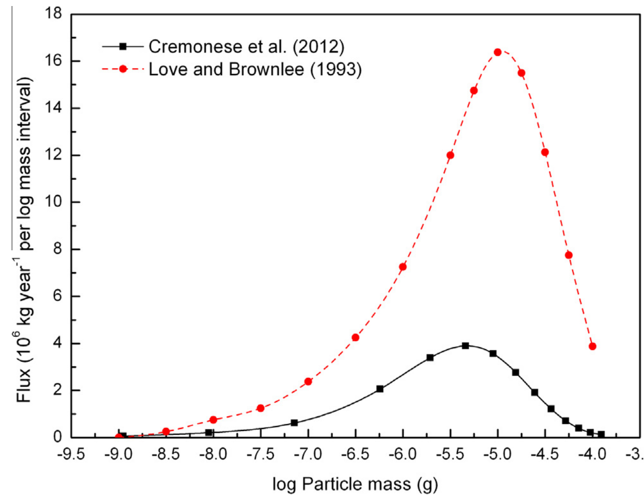

Fig. 1. Mass distribution of the annual flux of extraterrestrial material falling on Earth as stated by Love and Brownlee [20] (dashed red line) and Cremonese et al. [25] (black line). (For interpretation of the references to colour in this figure legend, the reader is referred to the web version of this article.)

4. Calculation of the expected production rate of extraterrestrial ^{41}Ca in IDPs

Two different approaches will be used to separately calculate the expected galactic (P_G) and solar (P_S) ^{41}Ca production rates. The first one will be obtained by comparison with the ^{53}Mn extraterrestrial production rate and the second one by applying the irradiation model of IDPs in interplanetary space described in the previous section.

4.1. Galactic production rate of ^{41}Ca: comparison with ^{53}Mn

Apart from ^{41}Ca ($T_{½} = 1.03 \times 10^5$ years), ^{53}Mn ($T_{½} = 3.68 \times 10^6$ years) is another long lived radionuclide which can be used to trace interplanetary dust on Earth. Like for ^{41}Ca, the most important source of extraterrestrial ^{53}Mn is by spallation on iron (>90%).

As stated by Eq. (1), the production rate of cosmogenic radionuclides depends on the relevant nuclear cross section as a function of energy $\sigma(E)$ and the flux of incident particles $\phi(E)$. When only cross sections at given energies are known instead of excitation functions for the formation of the respective nuclide from the target material, Eq. (1) can be approximated by Eq. (8). Therefore, this approximation will be used to estimate the galactic production rate of extraterrestrial ^{41}Ca by comparison with the production rate of ^{53}Mn.

$$P_i = \sum_j \int \frac{d\phi}{dE} \times N_j \times \sigma(j \to i, E) dE \approx \sum_j \sum_k (\phi(E_k) \times N_j \times \sigma(j \to i, E_k)) \quad (8)$$

If P_{Mn} and P_{Ca} are, respectively, the production rates of ^{53}Mn and ^{41}Ca as produced in IDPs by spallation on iron at GCR proton-energies in a determined range, the ratio between their production rates is then given by Eq. (9).

$$\frac{P_{Ca}}{P_{Mn}} \approx \frac{\sum_k (\phi(E_k) \times N_{Fe} \times \sigma_{Fe \to Ca}(E_k))}{\sum_k (\phi(E_k) \times N_{Fe} \times \sigma_{Fe \to Mn}(E_k))} \quad (9)$$

This ratio has been determined in the proton energy range 100–1500 MeV by using data of $^{nat}Fe(p,x)^{41}Ca$ and $^{nat}Fe(p,x)^{53}Mn$ reactions cross sections given by different authors [26,27] in addition to GCR proton fluxes at 1 AU [22,28], resulting in a value of 0.19 ± 0.05.

The feasibility of the estimation made with Eq. (9) has been tested by reproducing other ratios published by different authors using radionuclides which are also extraterrestrially formed and have their origin in spallation reactions involving iron isotopes. Fink et al. [16] have measured an average production $P(^{41}Ca)/P(^{36}Cl)$ ratio of 1.03 ± 0.04 in four small iron meteoroids and Nishiizumi and Caffe [32] determined this ratio as 1.01 ± 0.08. With the estimation explained in Eq. (9) and using the GCR proton fluxes from [22,28] and cross sections data for the reaction $^{nat}Fe(p,x)^{36}Cl$ from [26], this ratio has been calculated to be $P(^{41}Ca)/P(^{36}Cl) = 1.06 \pm 0.09$. Furthermore, Reedy [33] has estimated the ratio $P(^{36}Cl)/P(^{53}Mn)$ in very small stony objects by primary GCR at 1 AU to be 0.21, and with the above mentioned estimation this ratio was calculated to be 0.19 ± 0.03. For both cases, the estimations made using Eq. (9) are in good agreement with other published results, showing its validity.

Beryllium-10 can be used as a proxy for galactic ray produced ^{53}Mn, since its concentration in IDPs is also dominated by production due to galactic cosmic rays. Measurements of ^{10}Be in cosmic spherules [29,30] indicate a mean concentration of this radionuclide of 9 dpm kg^{-1}. Detailed data on element specific production rates of ^{10}Be, ^{26}Al and ^{53}Mn by galactic cosmic rays in meteoroids in depths of up to 500 g cm^{-2} have been published by Leya et al. [24]. Using this data and the elemental abundances in CI chondrites [31], depth dependent equilibrium activity ratios were calculated from 3.2 to 4.4 for $^{53}Mn/^{10}Be$ [24]. Using a mean equilibrium activity ratio of 3.8, the mean ^{53}Mn equilibrium concentration due to GCR production is estimated to be 34 dpm kg^{-1}. Using this mean ^{53}Mn equilibrium concentration and the ratio $P(^{41}Ca)/P(^{53}Mn)$ previously calculated results in a ^{41}Ca production rate due to galactic cosmic rays of 6.5 dpm kg^{-1}.

4.2. Solar production rate of ^{41}Ca: application of the irradiation model

In this section the solar component of the ^{41}Ca production rate will be calculated using the irradiation model explained in Section 3, by solving Eq. (7) numerically. Fig. 2 shows the solar production rates as a function of the IDPs' radii for some radionuclides with different half-lives, ranging from $T_{1/2} = 3.68 \times 10^6$ years for ^{53}Mn to $T_{1/2} = 5730$ years for ^{14}C, obtained by solving Eq. (7). For simplicity and direct visual comparison, the same production rate at 1 AU has been assumed for all radionuclides ($P_0 = 100$ dpm kg^{-1}). IDPs were assumed to be spherical with a density of 2.5 g cm^{-3}.

It has to be noticed that those radionuclides having shorter half-lives with respect to the exposure time (time of flight needed to travel from the Asteroid Belt at 3 AU to the Earth at 1 AU) reach a secular equilibrium and the measurement of the production rate at this equilibrium is equivalent to a measurement of the specific activity for this radioisotope. As stated in Eq. (3), this equilibrium production rate (specific activity) is the squared ratio of the distance that the IDPs have traveled, this means 1/9. This fact can be seen in Fig. 3, where the ratio between the production rates at 3 and 1 AU (P_{3AU}/P_{1AU}) for the radionuclides shown in Fig. 2 is represented.

For ^{41}Ca the decay constant has a value $\lambda = \ln(2)/T_{1/2} = 6.73 \times 10^{-6}\ y^{-1}$ and the solar production rate at 1 AU P_0 is calculated as follows: if the ^{41}Ca saturation activity of (24 ± 1) dpm kg^{-1} given by some authors [14–16] is assumed to be the sum of the galactic and solar components ($P_G + P_0$) at the Earth's orbit (1 AU), the solar component at 1 AU can be deduced

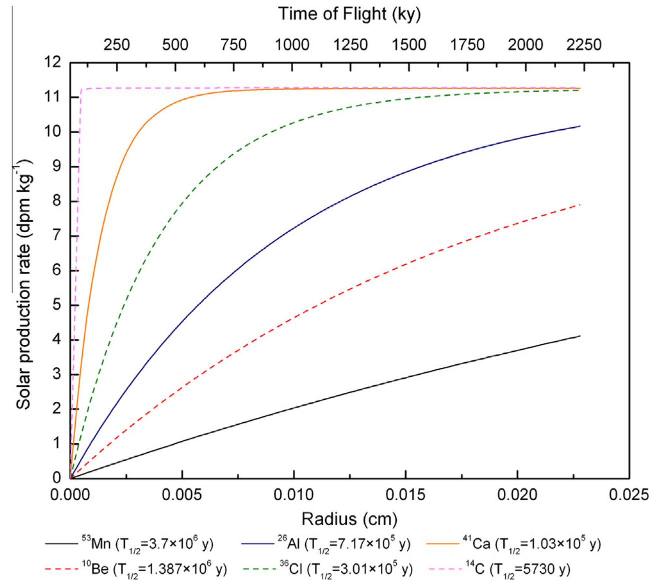

Fig. 2. Solar production rates of different radionuclides in IDPs with different radii, corresponding with the masses given by Cremonese et al. [25] and shown in Fig. 1 (black line) if a density of 2.5 g cm^{-3} is assumed. The corresponding time of flight given in the upper horizontal axis has been calculated using the Eq. (5). This production rate is equivalent to a specific (saturation) activity for those radionuclides which reach a secular equilibrium.

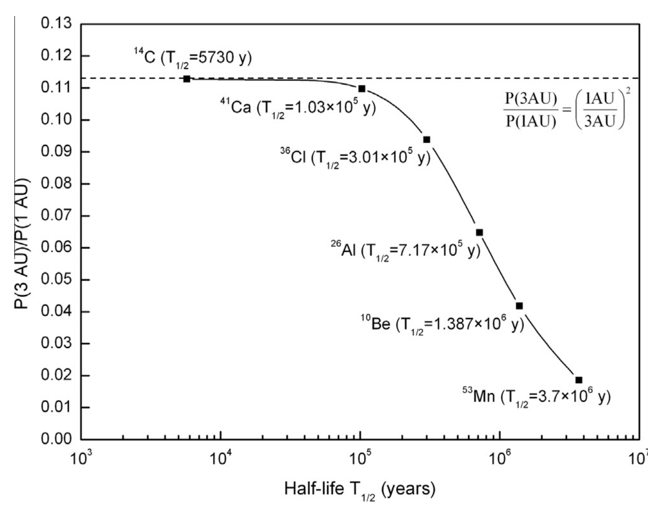

Fig. 3. Ratio between the production rates at 3 and 1 AU for radionuclides with different half-lives. It can be seen that those with the shortest half-lives reach an equilibrium value given by the dashed line which corresponds with the squared ratio between the distances, this means 1/9.

by subtracting the galactic component obtained in the previous section from this saturation activity. This allows us to calculate the solar component at 1 AU as $P_0 = (24 - 6.5)$ dpm kg^{-1} = 17.5 dpm kg^{-1}.

Using those two values to solve the differential equation given by Eq. (7), the solar production rate of ^{41}Ca for spherical IDPs with a density of 2.5 g cm^{-3} and the size distribution shown in Fig. 1 (black curve) [25] during their travel from the Asteroid Belt to the Earth can be calculated. This result is shown in Fig. 4. Then, by integration of the ^{41}Ca solar production rate (black line) over all particles' radii taking into account the contribution of each radius to the total terrestrial flux (red line, obtained from [25]), the weighted average solar production rate of ^{41}Ca in IDPs is 2 dpm kg^{-1}, which means 1/9 of the production rate at 1 AU estimated above (17.5 dpm kg^{-1}). This value is in good agreement with those published by Goswami et al. [34] of 2.5 and 2.3 dpm kg^{-1} for solar energetic particles with rigidity $R_0 = 100$ in targets of CI composition (this rigidity value may be a better representation of the average solar cosmic ray spectrum [35]) and also in agreement with calculated production rates of ^{41}Ca by solar protons in small meteorites given by Reedy [56].

Adding this solar production rate to the galactic component calculated in the previous section results in a total ^{41}Ca production rate in IDPs of 8.5 dpm kg^{-1}.

5. Annual accretion rate of extraterrestrial ^{41}Ca on the Earth

The mass accretion rate of IDPs on Earth (F_{IDP}) is an important tool to discriminate the extraterrestrial nature of the particles or isotopes found in different environments on the ground. In this context, the knowledge of the micrometeoroid flux arriving at our atmosphere is a key parameter for which different values have been found. Love and Brownlee [20] published a flux of meteoroids in the mass range 10^{-9} to 10^{-4} grams of (40,000 ± 20,000) tons per year by examination of hypervelocity impact craters on the space-facing end of the Long Duration Exposure Facility (LDEF) satellite, an orbital impact detector placed on a spacecraft for several years. This value agrees with the average extraterrestrial accretion rate over the past 80 million years of (37,000 ± 13,000) ton yr^{-1} derived from marine osmium [36]. Karner et al. [37] determined a rate of extraterrestrial accretion for particles in the size range 0.45 μm to ≈20 μm of (220 ± 110) tons per year from dust concentrates extracted from the Greenland Ice Sheet Project 2 (GISP2) ice core samples.

Taylor et al. [7] calculated a terrestrial accretion rate for 50–700 μm cosmic spherules of (1600 ± 300) ton yr^{-1} from micrometeoroids collected from the South Pole Water Well (SPWW) assuming a uniform global distribution. This rate is higher than the one estimated in deep-sea iron spherules corrected for post-deposition weathering of stony spherules (400–1200 ton yr^{-1}) [38]. The results from Taylor et al. [7] overlap other estimates [29,39] based on 5 and 14 spherules, respectively, extracted from well-dated Antarctic ice cores (1000–1500 ton yr^{-1}), and it falls within the broad range calculated by Peng and Lui [40] based on spherules extracted from deep-sea sediments (500–7000 ton yr^{-1}).

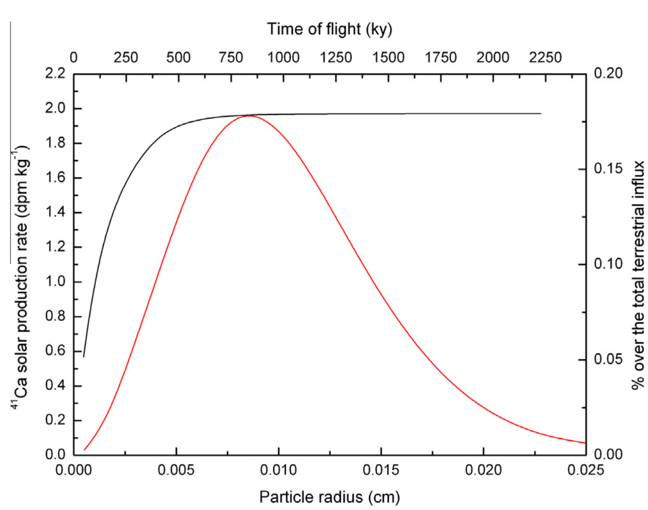

Fig. 4. ^{41}Ca solar production rate as a function of the particles' radii (black line) and contribution (in%) of every radii to the total terrestrial influx (red line). The red curve has been obtained from Cremonese et al. [25]. (For interpretation of the references to colour in this figure legend, the reader is referred to the web version of this article.)

Most recently, Gabrielli et al. [6] determined an average global extraterrestrial input during the Holocene of (78,000 ± 30,000) ton yr^{-1} by measuring Ir and Pt in 35 sections of ice cores from the European Greenland Ice-Core Project (GRIP). Cremonese et al. [25] have provided a new calibration of the flux of submillimeter particles impacting the Earth in the mass range from 10^{-9} to 10^{-4} grams of (7400 ± 1000) ton per year if the Asteroid Belt is assumed as the major source of dust. This was derived by computing a specific scaling law for impact craters on the Long Duration Exposure Facility. Those two last values are significantly lower than what was estimated by Love and Brownlee [20]. Karner et al. [37] have suggested that this could originate from the mass distribution used by Love and Brownlee (shown in Fig. 1) which may represent a systematic overestimate of particle masses as a consequence of the underestimation of impact velocities. For that reason the mass distribution given by Cremonese et al. [25] and also shown in Fig. 1 has been previously used in this work to calculate the solar production rate of ^{41}Ca by applying the irradiation model.

The accretion rate of ^{41}Ca ($F(^{41}Ca)$) can be then determined by Eq. (10), where F_{IDP} is the total mass influx, S_{earth} is the surface of the Earth in cm^2 and $N(^{41}Ca)$ is the ^{41}Ca production rate in IDPs previously calculated. If the most recent total mass influx of (7400 ± 1000 ton yr^{-1}) [25] is used in the calculation, this leads us to a value for the accretion rate of ^{41}Ca of (0.97 ± 0.13) atoms cm^{-1} yr^{-1}, although it could range from 0.03 to 10.2 atoms cm^{-1} yr^{-1} (corresponding to accretion rates of 220 and 78,000 ton yr^{-1}, respectively).

$$F(^{41}\mathrm{Ca}) = \frac{F_{IDP} \times N(^{41}\mathrm{Ca})}{S_{earth}} \qquad (10)$$

6. Calcium-41 as a tracer of interplanetary dust. Snow samples from Antarctica

Calcium-41, along with ^{53}Mn, is a key tracer for extraterrestrial material, as it has no significant terrestrial sources. On Earth, it is produced primarily by capture of thermal neutrons by ^{40}Ca at the surface. Other production modes, such as cosmic-rays interactions on ^{42,44}Ca, Ti and Fe, and atmospheric production might account for less than a few percent of the total amount of ^{41}Ca, and it is also limited to the top few meters of the Earth's surface [11]. After production, it decays via pure electron capture, emitting solely 3.3 keV K-shell X-rays of ^{41}K [16].

About 90% of the incoming mass of submillimeter extraterrestrial dust particles evaporates during atmospheric entry [7], their constituent minerals subsequently vaporize between an altitude of 80 and 120 km [8] and therefore, they can be measured by using aerosol and/or ice sampling techniques.

It has been demonstrated [41] that particles with radii smaller than 4 μm have falling times in the time scale of less than 100 days when only gravitation and Stokes-friction are taken into account. This value, compared to the typical time of flight for the IDPs (see Eq. (5)) between 10^4 and 10^6 years, means that production of radionuclides during the time between they enter the atmosphere and when they are accreted can be neglected. This, with the fact that ^{41}Ca has no significant terrestrial sources on Earth, means that in freshly deposited samples the atomic ratio ^{41}Ca/^{40}Ca measured by AMS would be equal to the ratio between the deposition rates as stated by Eq. (11), where $F(^{41}Ca)$ is the extraterrestrial ^{41}Ca flux due to the IDPs calculated in the previous section and $F(^{40}Ca)$ is the ^{40}Ca flux (deposition rate) at the sampling site.

$$\frac{F(^{41}\mathrm{Ca})}{F(^{40}\mathrm{Ca})} = \left[\frac{^{41}\mathrm{Ca}}{^{40}\mathrm{Ca}}\right] \quad (11)$$

Therefore the Antarctica is a good choice for a sampling site. Terrestrial contributions are minimized on account of its remoteness from continental sources. Due to its extremely low temperatures, the precipitated materials are perfectly preserved and do not diffuse. Calcium concentrations in snow from Antarctica show an inverse relationship with decreasing concentration at higher elevation [42]. In the vicinity of ice-free areas, such as the McMurdo Dry Valleys, Ca concentration is influenced from local sources. Elsewhere, the input is dominated by global dust input [43]. For example, a value for the ^{40}Ca deposition rate of 110 ng ^{40}Ca cm^{-2} yr^{-1} along the profile Mirny (66°30′S, 93°E, near the sea) which decreases by a factor of 5 at 500 km from the sea coast has been reported by Boutron et al. [44]. Another value of (22 ± 40) ng ^{40}Ca cm^{-2} yr^{-1} at (73°6.4′S, 165°27.8′E) near Antarctica's coast has also been reported [45]. Therefore, the ratio ^{41}Ca/^{40}Ca strongly depends on the selected sampling site, so selecting one site with small influx of natural ^{40}Ca would result in a higher extraterrestrial contribution to the ^{41}Ca/^{40}Ca ratio, the quantity measurable by AMS.

Besides extraterrestrially produced ^{41}Ca, also terrestrially produced ^{41}Ca exists in the ice samples. As mentioned before, the production of ^{41}Ca at the Earth's surface is mainly caused by thermal neutron capture ^{40}Ca(n,γ)^{41}Ca. This terrestrially produced ^{41}Ca concentration would represent, in principle, the natural background. The ^{41}Ca/^{40}Ca saturation value in calcareous rocks assuming that all thermal neutrons are captured by Ca and the absence of erosion has been measured to be 7×10^{-15} [11] in a tufa veneer from Egypt, a region characterized by low erosion and long exposure times [11]. Henning et al. [46] also measured a saturation ratio of $(7.6 \pm 4.5) \times 10^{-15}$ in surface limestone ($CaCO_3$) from the Grantsville limestone quarry in Utah (USA), although this ratio decreased to $(3.4 \pm 2.1) \times 10^{-15}$ in limestone sampled at 11 m depth, probably due to the fact that the neutron flux is nearly 10 times lower at a depth of 3 m than at the surface [11].

This means that considering the saturation value would not be an appropriate approach when erosion is not negligible, i.e. exhumation goes faster than the time needed to reach equilibrium. Consequently, for most of the terrestrial environments the equilibrium ^{41}Ca/^{40}Ca ratio could be considerably lower than these measured saturation values and, most importantly, would be strongly influenced by the local erosion rate of the sampling site. Different authors [14,47] have reported that only around 10% of the total thermal neutrons are captured by ^{40}Ca to undergo the reaction ^{40}Ca(n,γ)^{41}Ca in the lunar surface. If a similar assumption is used in the Earth's surface, the ^{41}Ca/^{40}Ca saturation values mentioned above could be even lower.

A snow sample collected near the Antarctic coast in an area having a deposition rate of (22 ± 40) ng ^{40}Ca cm^{-2} yr^{-1} [45] would have a ratio ^{41}Ca/^{40}Ca ranging $(0.09–3.09) \times 10^{-14}$, corresponding to accretion rates of ^{41}Ca of 0.03–10.2 atoms cm^{-1} yr^{-1}. Therefore, it can be clearly seen that the selection of the correct sampling site is very important, being mandatory to have a small influx of natural ^{40}Ca which prevents the dilution of the ^{41}Ca/^{40}Ca ratio.

For this work snow samples from two different locations in Antarctica were collected in order to measure the atom ratio ^{41}Ca/^{40}Ca and thus calculate the accretion rate of ^{41}Ca onto the Earth. The first sample, 1400 L of snow, was collected in 2011 from the Argentinean station Jubany, located on King George Island (62°14′S 58°40′O). Due to its proximity to the coast and its low altitude (10 mosl, meters over sea level), the concentration of ^{40}Ca was found to be very high (33 μg L^{-1}, measured by ICP-MS), in good agreement to values reported by Bertler [42] (between 20 and 30 μg L^{-1}). The mean annual precipitation rate in the Jubany station for the period 1995–2005 was 60 g cm^{-2} yr^{-1} [48]. Assuming accretion rates of ^{41}Ca of 0.03–10.2 at cm^{-1} yr^{-1}, this sample would deliver ^{41}Ca/^{40}Ca ratios of around $(0.006–2.06) \times 10^{-16}$, which could be actually below the natural background level of ^{41}Ca.

Bearing this fact in mind, a second snow sample (this time 400 L) will be collected in 2015 at the German station Kohnen (75°0′S, 0°4′E), located at around 750 km from shore and at an altitude of 2900 mosl. The mean annual precipitation rate in the Kohnen station is 6.4 g cm^{-2} yr^{-1} [49], a factor 10 lower than in the Jubany station. The expected ^{40}Ca concentration in this sample will also be lower than in the Jubany station (between 3 and 4 μg L^{-1}, as stated by Bertler [42]). So the overall total influx of natural ^{40}Ca will be lower, resulting in a higher ratio ^{41}Ca/^{40}Ca. Assuming accretion rates of ^{41}Ca in the range 0.03–10.2 atoms cm^{-1} yr^{-1}, this sample would deliver ^{41}Ca/^{40}Ca ratios of around $(0.81–265) \times 10^{-16}$, where the higher values should be above the natural background level of ^{41}Ca. These calculations highlight the importance of the selection of the correct sampling site.

The ^{41}Ca measurements will be performed at the Tandem Accelerator of the Technische Universität and the Maximilian Universität of München. Details of the set-up and performance of this facility for measurement of ^{41}Ca are described elsewhere [57]. The major challenge is the suppression of the ^{41}Ca isobar ^{41}K, made by preparing the samples as calcium hydride and selecting $^{41}CaH_3^-$ as beam from the sputter source. Basically, the analytical set-up on the high energy side of the accelerator consists of a time-of-flight measurement system for energy analysis, followed by the gas-filled magnet for isobar separation in conjunction with a multi cathode ionization chamber. With this setup, ^{41}K can be separated from ^{41}Ca on a level of ^{41}Ca/^{40}Ca = 10^{-15}.

7. Conclusions

Calcium-41 has been used for the first time as a tracer to calculate the amount of interplanetary dust accreted by the Earth per year. The measurement will be performed by AMS. Selected snow samples from the Antarctica should be suited for this determination.

Calcium-41 can be used as tracer for extraterrestrial material as it has very low terrestrial sources. Stable calcium concentrations in snow from the Antarctica vary from different sampling sites, increasing in sites with low elevation and located near the sea coast. It is important to have a small influx of natural ^{40}Ca in order to get a low terrestrial contribution to the ^{41}Ca/^{40}Ca ratio, the quantity measurable by AMS.

The first step of this study consisted to calculate the production rate of ^{41}Ca in IDPs accreted by the Earth due to the solar and galactic cosmic rays that interact with the bulk material during the traveling time from the area of formation (assumed to be the Asteroid Belt) to the Earth. For this calculation, an irradiation model with a galactic and a solar component has been used, leading to a production rate of ^{41}Ca in this extraterrestrial material of 8.5 dpm kg^{-1}. This production rate, used in accordance with the ^{41}Ca/^{40}Ca ratios that will be measured in snow samples from the Antarctica will serve to calculate the amount of extraterrestrial material accreted by the Earth per year.

References

[1] S.J. Kortenkamp, S.F. Dermott, Icarus 135 (1998) (1998) 469–495.
[2] D.E. Brownlee, Annu. Rev. Earth Planet. Sci. 13 (1985) 147–173.
[3] H.P. Robertson, Mon. Not. R. Astron. Soc. 97 (1934) 423–438.
[4] D.E. Brownlee, B. Bates, L. Schramn, Meteorit. Planet. Sci. 32 (1997) 157–175.

[5] L.S. Schramn, D.E. Brownlee, M.M. Wheelock, Meteorit. Planet. Sci. 24 (1989) 99–112.
[6] P. Gabrielli, C. Barbante, J.M.C. Plane, A. Varga, S. Hong, G. Cozzi, V. Gaspari, F.A.M. Planchon, W. Cairns, C. Ferrari, et al., Nature 432 (2004) 23–30.
[7] S. Taylor, J.H. Lever, R.P. Harvey, Nature 392 (1998) 899–903.
[8] S.G. Love, D.E. Brownlee, Icarus 89 (1991) 26–43.
[9] R. Trappitsch, I. Leya, Meteorit. Planet. Sci. 48 (2013) 195–210.
[10] M. Paul, I. Ahmad, W. Kutschera, Z. Phys. A 340 (1991) 249.
[11] D. Fink, J. Klein, R. Middleton, Nucl. Instrum. Meth. B 52 (1990) 572–582.
[12] R.C. Reedy, Proc. Lunar Planet. Sci. Conf. 38 (2007) 1192.
[13] C. Schnabel, H.A. Synal, P. Gartenmann, F.J. Santos-Arévalo, I. Gomez-Martinez, M. Suter, A. Tarabischi, T. Bastian, F. Sudbrock, U. Herpers, et al., Nucl. Instrum. Meth. B 223 (2004) 812–816.
[14] K. Nishiizumi, D. Fink, J. Klein, R. Middleton, J. Masarik, R.C. Reedy, Earth Planet. Sci. Lett. 148 (1997) 545–552.
[15] J. Klein, D. Fink, R. Middleton, S. Vogt, G.F. Herzog, Meteoritics 26 (1991) 358.
[16] D. Fink, J. Klein, R. Middleton, S. Vogt, G.F. Herzog, Earth Planet. Sci. Lett. 107 (1991) 115–128.
[17] D. Fink, M. Paul, G. Hollos, S. Theis, S. Vogt, R. Stueck, P. Englert, R. Michel, Nucl. Instrum. Meth. B 29 (1987) (1987) 275–280.
[18] J.T. Wasson, G.W. Kallemeyn, Philos. T. Roy. Soc. A 325 (1988) 535–544.
[19] K.C. Welten, D.J. Hillegonds, J. Masarik, K. Nishiizumi, Nucl. Instrum. Meth. B 259 (2007) 653–662.
[20] S.G. Love, D.E. Brownlee, Science 262 (1993) 550–553.
[21] R. Michel, M. Lüpke, U. Herpers, R. Rösel, M. Suter, B. Dittrich-Hammen, P.W. Kubik, D. Filges, P. Cloth, Planet. Space Sci. 43 (1995) 557–572.
[22] R.M. Auer, Applications of ^{26}Al in atmospheric research (Ph.D. thesis), University of Wien, 2008.
[23] J.A. Burns, P.L. Lamy, S. Soter, Icarus 40 (1979) 1–48.
[24] I. Leya, H.J. Lange, S. Neumann, R. Wieler, R. Michel, Meteorit. Planet. Sci. 35 (2000) 259–286.
[25] G. Cremonese, P. Borin, E. Martellato, F. Marzari, M. Bruno, Astrophys. J. Lett. 749 (2012) L40.
[26] C. Villagrasa-Canton, A. Boudard, J.-E. Ducret, B. Fernandez, S. Leray, C. Volant, P. Armbruster, T. Enqvist, F. Hammache, K. Helariutta, et al., Phys. Rev. C 75 (2007) 044603.
[27] S. Merchel, T. Faesterman, U. Herpers, K. Knie, G. Korschinek, I. Leya, R. Michel, G. Rugel, A. Wallner, Nucl. Instrum. Meth. B 172 (2000) 806–811.
[28] J.Z. Wang, E.S. Seo, K. Anraku, M. Fujikawa, M. Imori, T. Maeno, N. Matsui, H. Matsunaga, M. Motoki, S. Orito, et al., Astrophys. J. 564 (2002) 244–259.
[29] F. Yiou, G.M. Raisbeck, Meteoritics 22 (1987) 539–540.
[30] K. Nishiizumi, J.R. Arnold, D.E. Brownlee, M.W. Caffee, R.C. Finkel, R.P. Harvey, Meteoritics 30 (1995) 728–732.
[31] E. Anders, N. Grevesse, Geochim. Cosmochim. Acta 53 (1989) 197–214.
[32] K. Nishiizumi, M.W. Caffee, Meteorit. Planet. Sci. 33 (1998) A117.
[33] R.C. Reedy, Proc. Lunar Planet. Sci. Conf. 21 (1990) 1001.
[34] J.N. Goswami, K.K. Marhas, S. Sahijpal, Astrophys. J. 549 (2001) 1151–1159.
[35] R. Michel, Radiochim. Acta 87 (1999) 47–73.
[36] B. Peuker-Ehrenbrink, Geochim. Cosmochim. Acta 60 (1996) 3187–3196.
[37] D.B. Karner, J. Levine, R.A. Muller, F. Asaro, M. Ram, M.R. Stolz, Geochim. Cosmochim. Acta 67 (2003) 751–763.
[38] M.T. Murrell, P.A. Davis, K. Nishiizumi, H.T. Millard, Geochim. Cosmochim. Acta 44 (1980) 2067–2074.
[39] F. Yiou, G.M. Raisbeck, C. Jehanno, Meteoritics 24 (1989) 344.
[40] H. Peng, Z. Lui, Meteoritics 24 (1989) 315.
[41] T. Schätz, 53Mn in extraterrestricher Materie (Diploma Thesis), Technische Universität München, 1997.
[42] N. Bertler, Ann. Glaciol. 41 (2005) 167–179.
[43] A. Aristarain, R. Delmas, Atmos. Environ. 36 (2002) 765–772.
[44] C. Boutron, M. Echevin, C. Lorius, Geochim. Cosmochim. Acta 36 (1972) 1029–1041.
[45] G. Ghermandi, P. Laj, M. Capotoso, R. Cecchi, C. Riotinto, Nucl. Instrum. Meth. B 150 (2000) 392–397.
[46] W. Henning, W.A. Bell, P.J. Billquist, B.G. Glagola, W. Kutschera, Z. Liu, H.F. Lucas, M. Paul, K.E. Rehm, J.L. Yntema, Science 236 (1987) 725–727.
[47] R.C. Reedy, Proc. Lunar Planet. Sci. Conf. 9 (1978) 2961–2984.
[48] A. Curtosi, E. Pelletier, C.L. Vodopivez, W.P. Mac Cormack, Sci. Total Environ. 383 (2007) 193–204.
[49] EPICA Community Members, Nature 444 (2006) 195–198.
[50] M. Paul, D. Fink, P. Englert, S. Theis, Meteoritics 20 (1985) 726–727.
[51] P.W. Kubik, D. Elmore, N.J. Conrad, K. Nishiizumi, J.R. Arnold, Nature 319 (1986) 568–570.
[52] G. Korschinek, H. Morinaga, E. Nolte, E. Preisenberg, U. Ratzinger, A. Urban, P. Dragovitsch, S. Vogt, Nucl. Instrum. Meth. B 29 (1987) 67–71.
[53] D. Fink, J. Klein, R. Middleton, S. Vogt, G.F. Herzog, R.C. Reedy, Geochim. Cosmochim. Acta 62 (1998) 2389–2402.
[54] G.F. Herzog, A. Albrecht, P. Ma, D. Fink, J. Klein, R. Middleton, D.D. Bogard, L.E. Nyquist, C.Y. Shih, D.H. Garrison, Y. Reese, J. Masarik, R.C. Reedy, G. Rugel, T. Faestermann, G. Korschinek, Meteorit. Planet. Sci. 46 (2011) 284–310.
[55] K. Nishiizumi, J.R. Arnold, D. Fink, J. Klein, R. Middleton, Meteoritics 26 (1991) 379.
[56] R.C. Reedy, Proc. Lunar Planet. Sci. Conf. 42 (2011) 2365.
[57] A. Wallner, A. Arazi, T. Faestermann, K. Knie, G. Korschinek, H.J. Maier, N. Nakamura, W. Rühm, G. Rugel, Nucl. Instrum. Meth. B 223–224 (2004) 759–764.